Eur. Phys. J. B **20**, 335–341 (2001)

THE EUROPEAN PHYSICAL JOURNAL B

EDP Sciences

Time-domain interferometry using synchrotron radiation applied to diffusion in ordered alloys

M. Kaisermayr[1,a], B. Sepiol[1], H. Thiess[1,2], G. Vogl[3,1], E.E. Alp[4], and W. Sturhahn[4]

[1] Institut für Materialphysik, Universität Wien, 1090 Wien, Austria
[2] European Synchrotron Radiation Facility, 38043 Grenoble, France
[3] Hahn-Meitner Institut, 14109 Berlin, Germany
[4] Advanced Photon Source, 9799 Argonne, IL, USA

Received 21 September 2000 and Received in final form 13 December 2000

Abstract. Time-domain interferometry of synchrotron radiation (TDI) has recently been used as a tool for investigating diffusion in glasses. This work deals with an extension of this technique to ordered structures. In a TDI experiment performed on the $B2$ alloy CoGa at the APS the intensity scattered into Bragg directions showed no detectable quasielastic signal. Experimental lower limits of the elastic contribution are given. They are in accordance with the coherent scattering function derived in this paper. This result indicates that TDI can be applied to diffusion in crystalline solids, *e.g.* intermetallic alloys, by using *diffuse* scattering. Requirements and limitations of diffuse scattering experiments are discussed.

PACS. 66.30.Fq Self-diffusion in metals, semimetals, and alloys – 76.80.+y Mössbauer effect; other gamma-ray spectroscopy – 61.72.Ji Point defects (vacancies, interstitials, color centers, etc.) and defect clusters

1 Introduction

Atomistic methods are important tools for studies of the microscopic diffusion mechanism in complex crystalline materials like intermetallic alloys as they allow to determine the frequencies and direction of atomic jumps [1]. Up to now three methods using quasielastic effects have been successfully applied to study self diffusion in intermetallic alloys: Quasielastic Mössbauer spectroscopy (QMS) [2], nuclear resonant scattering (NRS) [3] and quasielastic neutron scattering (QNS) [4]. Whereas QMS and NRS are practically limited to ^{57}Fe for diffusion studies in crystalline solids, the applicability of QNS is restricted to fast diffusers due to the comparably low energy resolution of currently available backscattering spectrometers (μeV compared with neV for QMS and NRS). Even neutron spin-echo spectrometry is not able to compete with Mössbauer spectroscopy at the momentum transfers which are required in order to investigate diffusion processes on the atomic scale.

A method based on the Mössbauer effect, but using the powerful features of synchrotron radiation is time domain interferometry of synchrotron radiation (TDI). The main advantage of this technique is given by the fact that it does not require resonant Mössbauer nuclei and therefore offers an *a priori* unlimited choice of targets. A detailed description of this method can be found in a paper of Baron *et al.* [5]. Essentially, TDI consists in extracting the intermediate scattering function, $S(\mathbf{q},t)$, and therewith the atomic correlation function, $G(\mathbf{r},t)$, from the interference of a reference wave with a wave scattered by the diffusing atoms. The two waves are created by instantaneous excitation of two targets containing ^{57}Fe atoms – one before and one behind the sample. One of the two targets is kept in constant motion, which results in a small relative energy shift leading to a beat pattern with a well defined frequency Ω. These beats are disturbed by quasielastic scattering, which is described by the intermediate scattering function. The experimental setup is schematically shown in Figure 1. According to Baron *et al.* [5] $S(\mathbf{q},t)$

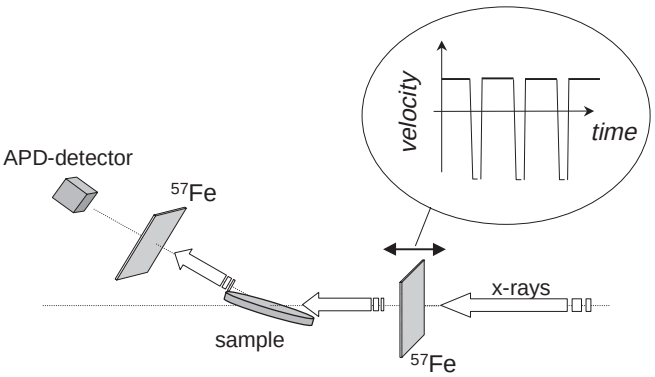

Fig. 1. Experimental setup. The insert shows schematically the time dependence of the velocity of the stainless-steel foil positioned upstream relative to the sample.

[a] e-mail: kaiserm@ap.univie.ac.at

is related to the momentum-time differential cross section *via*

$$(\frac{\partial^2\sigma}{\partial\mathbf{q}\partial t})_{\rm coh} \propto [1 + f_{\rm DW}(\mathbf{q})\cos(\Omega t)\, S(\mathbf{q},t)], \qquad (1)$$

where, $f_{\rm DW}$ stands for the Debye-Waller factor.

The first TDI experiment has been performed on the glassy system glycerol [5]. However, the great interest in investigations of diffusion mechanisms in intermetallic compounds like NiAl, Ni_3Al, TiAl, etc., which are not accessible to the microscopic methods cited above, makes an adaptation of TDI to crystalline solids particularly promising. Ruebenbauer and Wdowik [6] recently proposed to investigate the time dependence of the intensity of Mössbauer radiation scattered into *Bragg reflections* by intermetallic alloys (hence non-Bravais lattices). While this procedure of course provides the highest intensities, there are some problems associated to it, regarding the proportion of the quasielastic contribution observable in these directions. A simple picture suggests that scattering from *Bravais* lattices into Bragg directions shows no quasielastic effects since wave parts are scattered from different lattice sites without relative phase shifts [7]. In the same simple picture, the problem is considerably more subtle for *non-Bravais* lattices – especially for superlattice peaks where the different parts of the wave scattered by atoms jumping between different sublattices are no longer in phase but show relative phase shifts, *e.g.*, phase shift π for nearest-neighbour jumps on a $B2$ lattice. This subtlety is illustrated by the fact that the incoherent scattering function, $S_{\rm inc}(\mathbf{q},t)$, is *elastic* at reciprocal lattice points corresponding to *fundamental* Bragg reflections and *quasielastic* in reciprocal lattice points corresponding to *superlattice* reflections. This paper is set out to determine experimentally at which point TDI in Bragg directions might be used for diffusion studies in crystalline alloys. Furthermore, we will derive the coherent scattering function for the discussed case using the Van Hove formalism [8]. This will be done for Bragg reflections as well as for diffuse scattering due to lattice disorder.

2 Experiment

We have applied the TDI technique to diffusion in the intermetallic alloy CoGa. The experiment was performed at the beamline 3ID at the Advanced Photon Source (APS, Argonne National Laboratories). Preliminary results have been published in reference [9] without a detailed interpretation.

2.1 Sample

The experiment was performed on a CoGa single crystal with 62.7(5) at.% Co which was cut parallel to the $\langle 100\rangle$ lattice plane. CoGa crystallizes in the $B2$ structure and exhibits triple defects [10]. The lattice constant [11] is 2.875 Å at 1173 K. Since the composition is far from stoichiometry, a high degree of disorder, mainly due to the presence of Co atoms on the Ga sublattice, is expected. QNS experiments [12] showed that Co atoms diffuse *via* jumps between nearest neighbour sites. Tracer experiments indicate that Ga diffusion is several times slower than Co diffusion [13]. While these measurements point towards jumps to next-nearest neighbour sites, QNS experiments [14,15] on the very similar $B2$ alloy NiGa indicate NN jumps for Ga. We have accounted for this uncertainty of the Ga diffusion in the data treatment.

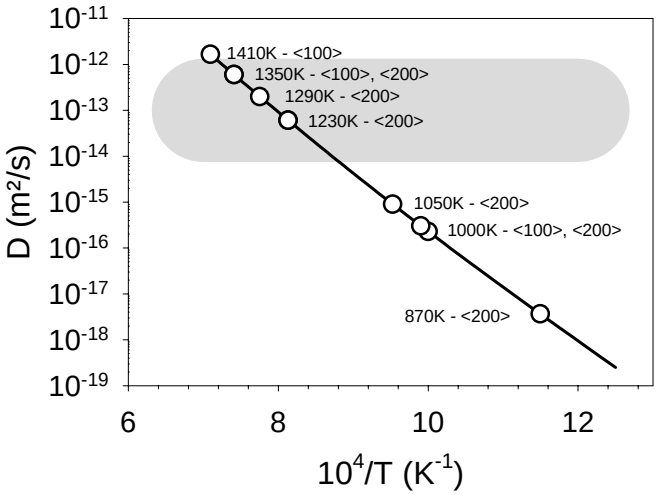

Fig. 2. Lines: Arrhenius plot of Co diffusion coefficients in $Co_{60}Ga_{40}$ according to reference [13]. Circles: Points corresponding to the temperatures where the TDI measurements at the $\langle 100\rangle$ and $\langle 200\rangle$ reflection were carried out. The shaded area indicates the region of diffusivities where the residence times of the atoms on the lattice sites are comparable to the lifetime of the ^{57}Fe excitation. Points corresponding to measurements at temperatures below 870 K are not shown in this diagram.

2.2 Experimental setup

During the experiment at the beamline 3ID, the APS storage ring was operated in the 'timing mode' which provides a single bunch every 153 ns. The undulator was tuned to the ^{57}Fe transition at 14.4 keV. The high resolution monochromator allowed to select a 2 meV bandwidth. The temperature was chosen such that the relaxation time τ of Co diffusion is of the same order of magnitude as the lifetime of the excited state of the ^{57}Fe Mössbauer nuclei (141 ns). Figure 2 shows the diffusion constants of Co for the temperatures where TDI measurements have been carried out, compared to the range of diffusivities which is convenient for Mössbauer experiments due to the comparability of τ to the Mössbauer lifetime. The diffusion constants for both constituents of CoGa have been taken from Stolwijk *et al.* [13]. The measurements at lower temperatures were carried out in order to determine the diffusion-independent parameters for the fitting procedure.

The experimental setup is sketched in Figure 1. We used two stainless-steel foils with thicknesses of 1.03 μ and 1.08 μ, respectively. The foil upstream relative to

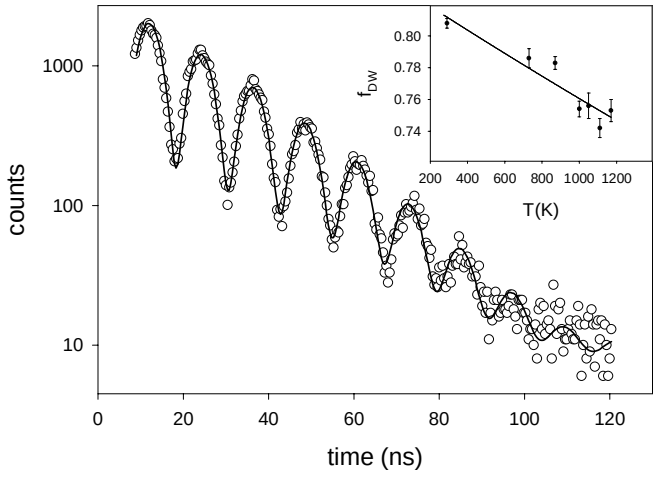

Fig. 3. Time dependence of the count rate in the ⟨200⟩ Bragg reflection at room temperature. Line: Time dependence according to equation (1). Insert: Temperature dependence of the Debye-Waller factor for the ⟨200⟩ spectra at lower temperatures. Line: Debye-model.

the sample position was moved at a constant velocity of about 7.2 mm/s at a frequency of 11 Hz. This produced a frequency shift between the two foils corresponding to one beat every 12.2 ns, respectively $\Omega = 0.515$ ns^{-1}. An avalanche photo diode detector provided a resolution under 1 ns starting approximately 20 ns after the bunch. Two high temperature furnaces were used – one allowing measurements in Bragg geometry, *i.e.*, backscattering and the second one for Laue geometry, *i.e.*, transmission. Count rates in transmission geometry were considerably higher, probably due to less absorption losses. The temperature calibration of the furnaces was carried out using the isomer shift of iron.

We measured the time dependence of the intensity in the ⟨100⟩ reflection which is of superlattice type and the ⟨200⟩ reflection which is fundamental. Measurements were performed at 290, 730, 870, 1000, 1050, 1110, 1170, 1230, 1290 and 1350 K for the ⟨200⟩ reflection and 290, 1000, 1010, 1230, 1350 and 1410 K for the ⟨100⟩ reflection. Because of the very similar form factors of Co and Ga atoms the count rates in the superlattice peak were significantly lower than in the fundamental peak. The resonant count rates were typically between some 100 Hz (fundamental peak at RT) and 1 Hz or less (superlattice peak at 1350 K). The room temperature spectrum of the ⟨200⟩ reflection is shown in Figure 3.

Special care was taken to avoid vibrations, *e.g.* from the vacuum pump of the high temperature furnace. However, there remained vibrations leading to a decrease of the beat amplitude with time – even at room temperature. These vibrations have been taken into account *via* a Gaussian shaped frequency distribution with width σ_Ω. An additional smearing-out of the interference pattern at all temperatures may arise from variations of the effective thickness L of the stainless steel foils which has been taken into account in the fit *via* a Gaussian shaped thickness distribution with width σ_L.

2.3 Data treatment

All spectra that were taken at temperatures where diffusion is relevant ($T \geq 1230$ K) were fitted with a sum of a purely elastic and a purely quasielastic component. The quasielastic component was approximated by an exponential decay with relaxation time $\bar{\tau}$, the latter being calculated from the diffusion constants of Stolwijk *et al.* [13] *via* $\bar{\tau} = l^2/(6D)$ where l denotes the jump length for NN-jumps on a $B2$ lattice. The elastic contribution is indicated by the coefficient η where $\eta = 1$ denotes completely elastic scattering and $\eta = 0$ completely quasielastic scattering. It is important to note that the measured elastic contribution, η, may hide a quasielastic contribution which might not be detectable due to the comparably slow Ga diffusion. One therefore has to account for the fact that a considerable part of the experimentally found elastic contribution may in reality be quasielastic scattering from Ga with its long relaxation times. We do this by introducing a corrected lower limit for elastic scattering, denoted with $\epsilon_{\min}$, instead of the experimental lower limit, $\eta_{\min}$. The measured elastic contribution η then contains the elastic part, ϵ, as well as a term which takes into account the hidden quasielastic scattering from Ga atoms and a quasielastic part with relaxation time $\bar{\tau}$ from diffusing Co atoms. The intermediate scattering function reads

$$S(t) \propto \eta + (1-\eta)\exp(-\frac{t}{\bar{\tau}}) = \epsilon + (1-\epsilon)I_{\mathrm{Ga}} + (1-\epsilon)I_{\mathrm{Co}}\exp(-\frac{t}{\bar{\tau}}), \quad (2)$$

where the relative contributions I_{Co} and I_{Ga} are proportional to the respective atomic form factors and concentrations and scaled to $I_{\mathrm{Co}} + I_{\mathrm{Ga}} = 1$. By having assumed the relaxation time corresponding to Ga diffusion to be infinitely long, we have made the most careful choice regarding the lower limit $\epsilon_{\min}$, which will be the main result of this paper. An eventual undetected quasielastic contribution from Ga is then contained in the term $(1-\epsilon)I_{\mathrm{Ga}}$ so that the total measured elastic contribution is assumed to be $\eta = \epsilon + (1-\epsilon)I_{\mathrm{Ga}}$. In this way uncertainties regarding the exact Ga diffusion mechanism are taken into account.

For each fit of the high temperature spectra the amplitude, the background and the beat frequency, Ω, were refined while the parameters L, σ_Ω, σ_L and f_{DW} which are correlated to η were fixed during the fit. The effective thickness, L, of the stainless steel foils was fixed to the average value, $L = 17.5$, obtained in the fits of the low temperature spectra. While the simulated spectra were very sensitive to changes in the width of the frequency distribution, σ_Ω, the dependence of χ^2 from the thickness distribution σ_L turned out to be rather weak. σ_Ω was fixed to the average values of the low temperature spectra, $\sigma_\Omega/\Omega = 0.024$, while σ_L was estimated to $\sigma_L = 0.8$. The Debye-Waller factor, f_{DW}, was extrapolated from low temperature measurements of the ⟨200⟩ reflection (see insert of Fig. 3) to the values given in Table 1 by using the Debye approximation.

Table 1. Estimated relaxation times $\bar{\tau}$, extrapolated Debye-Waller factor f_{DW} as well as the lower limits for the elastic contribution $\eta_{\min}$ (raw) and $\epsilon_{\min}$ (corrected value) for the relevant high temperature spectra.

T(K)	reflection	$\bar{\tau}$ (ns)	f_{DW}	$\eta_{\min}$	$\epsilon_{\min}$
1350	⟨100⟩	19.5	0.808	0.86	0.75
1410	⟨100⟩	6.0	0.807	0.72	0.49
1230	⟨200⟩	182	0.745	0.92	0.85
1290	⟨200⟩	51	0.741	0.96	0.93
1350	⟨200⟩	19.5	0.737	0.97	0.94

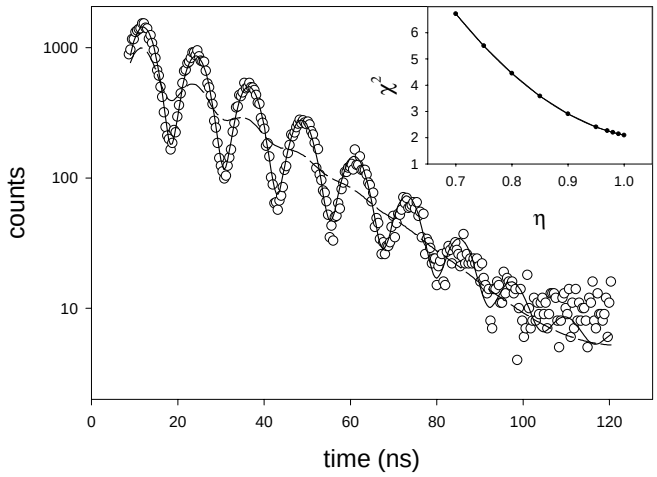

Fig. 4. Time dependence of the count rate in the ⟨200⟩ Bragg reflection at 1350 K. Lines: Time dependence according to equations (1) and (2) assuming $\eta = 0$ (solid) and $\eta = 1$ (dashed). Insert: Dependence of χ^2 as a function of η for this spectrum.

The double differential cross-section, equation (1), with the intermediate scattering function, equation (2), were then fitted to the high temperature spectra for different values of η. The best fits to the two extreme cases, $\eta = 1$ and $\eta = 0$, are shown in Figure 4 for the ⟨200⟩ and Figure 5 for the ⟨100⟩ reflection, both at 1350 K. From each fit we have calculated a χ^2 value in order to determine the sensitivity of the experimental spectra to elastic and quasielastic scattering, respectively. Two of those plots are shown in the inserts of Figures 4 and 5.

2.4 Results

For all spectra the minimum of χ^2 was found to be close to $\eta = 1$. The minimum was sharpest for those spectra with good statistics and short relaxation times $\bar{\tau}$. For each spectrum a lower limit, $\eta_{\min}$, for the experimentally determinable elastic contribution was calculated as follows: In those cases where the value of η_0 corresponding to the minimum of the χ^2 parabola was smaller than unity, a 99% confidence band, $\Delta\eta$, was subtracted from η_0, hence $\eta_{\min} = \eta_0 - \Delta\eta$. For the spectra where $\eta_0 > 1$, we assumed $\eta_{\min} = 1 - \Delta\eta$.

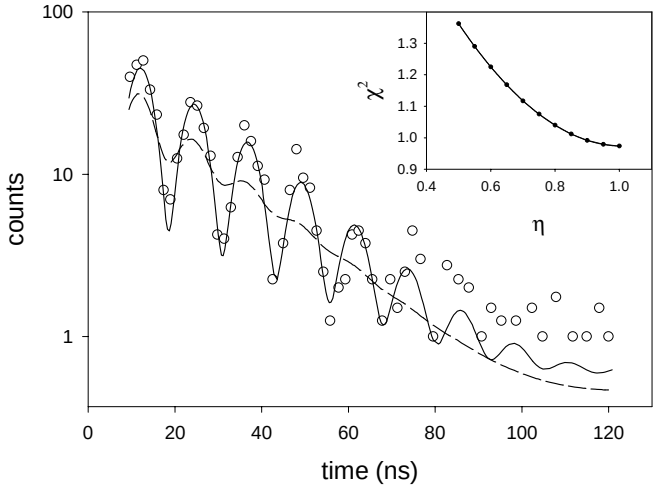

Fig. 5. Time dependence of the count rate in the ⟨100⟩ Bragg reflection at 1350 K. Lines: Time dependence according to equations (1) and (2) assuming $\eta = 0$ (solid) and $\eta = 1$ (dashed). In order to improve the readability of the figure, four channels compared to Figures 3 and 4 were grouped together. Insert: Dependence of χ^2 as a function of η for this spectrum.

The lower limit for the elastic contribution, $\eta_{\min}$, was found to be 0.86 for the ⟨100⟩ reflection and 0.97 for the ⟨200⟩ reflection (see Tab. 1). However, as already mentioned above, the experimentally found elastic contribution may hide a quasielastic part with long relaxation times corresponding to the slow Ga diffusion. This was taken into account by subtracting from unity the term $(1-\eta)(I_{\mathrm{Co}} + I_{\mathrm{Ga}})/I_{\mathrm{Co}}$. This yields the corrected lower limit for elastic scattering, $\epsilon_{\min}$. Finally, we get the following results: $\epsilon_{\min} = 0.75$ for the ⟨100⟩ reflection and $\epsilon_{\min} = 0.94$ for the ⟨200⟩ reflection.

3 Interpretation

Our experiment indicates that the intensity scattered into Bragg reflections is mainly elastic, in fundamental as well as in superlattice reflections. This is in accordance with the following derivation of the coherent scattering factor using the Van Hove formalism:

An exact expression for the intermediate scattering function for self diffusion *via* vacancies in intermetallic alloys can be obtained by Fourier transformation of the pair correlation function $G(\mathbf{r}, t)$ which is the sum of the pair correlation functions $G_i^j(\mathbf{r}, t)$ defined separately referring to different sublattices, i and j, multiplied with c_j, the concentration of the scattering element on the jth sublattice:

$$G(\mathbf{r}, t) = \sum_{i,j} c_j G_i^j(\mathbf{r}, t). \tag{3}$$

For a detailed definition of $G_i^j(\mathbf{r}, t)$ see reference [16]. Instead of one rate equation – as in the Chudley-Elliott model for Bravais lattices [17] – we have to deal with a

Table 2. Properties of scattering into selected points in reciprocal space. The incoherent scattering function, $S_{\mathrm{inc}}(\mathbf{q},t)$, according to Randl *et al.* [20], the coherent scattering function, $S(\mathbf{q},t)$, according to equation (4). The following abbreviations are used: el.: elastic; qe.: quasielastic; diff.: diffuse.

	Bravais		non Bravais	
	$S(\mathbf{q},t)$	$S_{\mathrm{inc}}(\mathbf{q},t)$	$S(\mathbf{q},t)$	$S_{\mathrm{inc}}(\mathbf{q},t)$
fundamental	el.	el.	el.+(diff.,qe.)	el.
superlattice	–	–	el.+(diff., qe.)	qe.
off Bragg	diff., qe.	qe.	diff., qe.	qe.

set of rate equations which can be solved using the so called jump matrix [18–20] which contains the vectors and frequencies corresponding to jumps between the different sublattices.

A somewhat lengthy but straightforward calculation (please see again Ref. [16]) yields:

$$S(\mathbf{q},t) = \sum_p w'_p \exp(M_p t) + N \sum_{\mathbf{G}} \delta(\mathbf{q}-\mathbf{G}) \sum_{i,j} c_i\, c_j\, \exp(\mathrm{i}\mathbf{q}\mathbf{l}_i^j), \quad (4)$$

where M_p denotes the pth eigenvalue of the jump matrix, $\mathbf{G}$ is a reciprocal lattice vector and w'_p are weighting factors,

$$w'_p = \sum_{i,j} (1-c_j)\sqrt{c_i c_j}(\mathbf{b}^p)_i (\mathbf{b}^{p*})_j, \quad (5)$$

where $\mathbf{b}_i^p$ denotes the ith component of the pth eigenvector of the jump matrix.

$S(\mathbf{q},t)$ consists of a time dependent term describing isotropic diffuse scattering and a term containing Bragg scattering which is time independent. Hence – apart from a negligible contribution of diffuse scattering – no time dependence can be expected in Bragg directions. This is exactly what has been observed in the experiment. An overview over the scattering properties according to equation (5) compared to incoherent scattering is given in Table 2. Note, that equation (4) is valid only for non-Bravais lattices which are occupied by one type of scattering atoms only – of course an unrealistic case for X-ray scattering. However, as is shown in Appendix A, the situation remains qualitatively unchanged if the lattice is occupied by more than one scattering element: All interferences between atoms of different elements are contained in a Bragg term which is strictly time independent.

4 TDI using diffuse scattering

The first term on the right hand side of equation (4) describes diffuse scattering due to lattice disorder. This term is time dependent and therefore diffuse scattering appears in principle suitable for diffusion studies in intermetallic alloys using TDI. Please note, that since the weights of the exponentials in equation (5) contain a term $(1-c_j)$ the absolute intensity vanishes for perfectly ordered lattices. However, intermetallic compounds usually exhibit defect concentrations up to several percent at temperatures relevant for diffusion studies and are therefore expected to show quasielastic diffuse scattering, due to partial site occupation. This effect can further be enhanced by going to off-stoichiometric compositions.

An example of the intermediate scattering function for a $B2$ structure is shown in Figure 6. The intermediate scattering function in this case is a sum of two exponential decays,

$$S(t) \propto w'_1 \exp(-M_1 t) + w'_2 \exp(-M_2 t), \quad (6)$$

the relative weights, w_i, and decay rates, M_i, of which are shown as a function of the momentum transfer $\mathbf{q}$. The lattice constant was assumed to be 3 Å, *i.e.* similar as in systems like CoGa, FeAl or NiAl. Both sublattices shall be partially occupied by the same element with occupation probabilities $c_1 = 0.7$ and $c_2 = 0.3$, respectively. A derivation of S($\mathbf{q}$,t) for $B2$-lattices can be found in the Appendix B.

Figure 6 shows the following general features of S($\mathbf{q}$,t): For reciprocal lattice points corresponding to fundamental peaks the weight, w'_2, of the fast exponential decay equals zero and the remaining part with weight $w'_1 = 1$ has $M_1 = 0$, hence is entirely elastic. For superlattice peaks the fast decay has a finite weight corresponding to coherent diffuse scattering. However, the scattered intensity is *still mainly elastic* because the intensity of the broad line is small compared to the intensity of the elastic line.

The regions between the reciprocal lattice points correspond to quasielastic diffuse scattering due to lattice disorder. The largest differences in the diffusion induced decay rates of the intermediate scattering function are found near the reciprocal lattice points. However, it is not advisable to measure at these positions *exactly* since the diffuse intensity will be covered by elastic Bragg scattering.

The values in Figure 6 are calculated for a *single* scattering element. For more than one element the contributions of the different types of atoms simply add up as is shown in the Appendix A.

Since the intensities of diffuse scattering are in general very low, large detectors with sufficient time resolution will be required in order to cover a solid angle as large as possible. Also, could the intensity be concentrated on a small detector by using focussing optics. In order to avoid Debye-Scherrer rings the use of single crystalline samples will be indispensable. Still, the main experimental difficulty will be low count rates. However, the advances which have been achieved in the recent years in the fields of undulator techniques and high resolution monochromators give rise to hope for an early application of TDI to the investigation of diffusion in intermetallic alloys, thus opening a wide range of materials for direct diffusion studies.

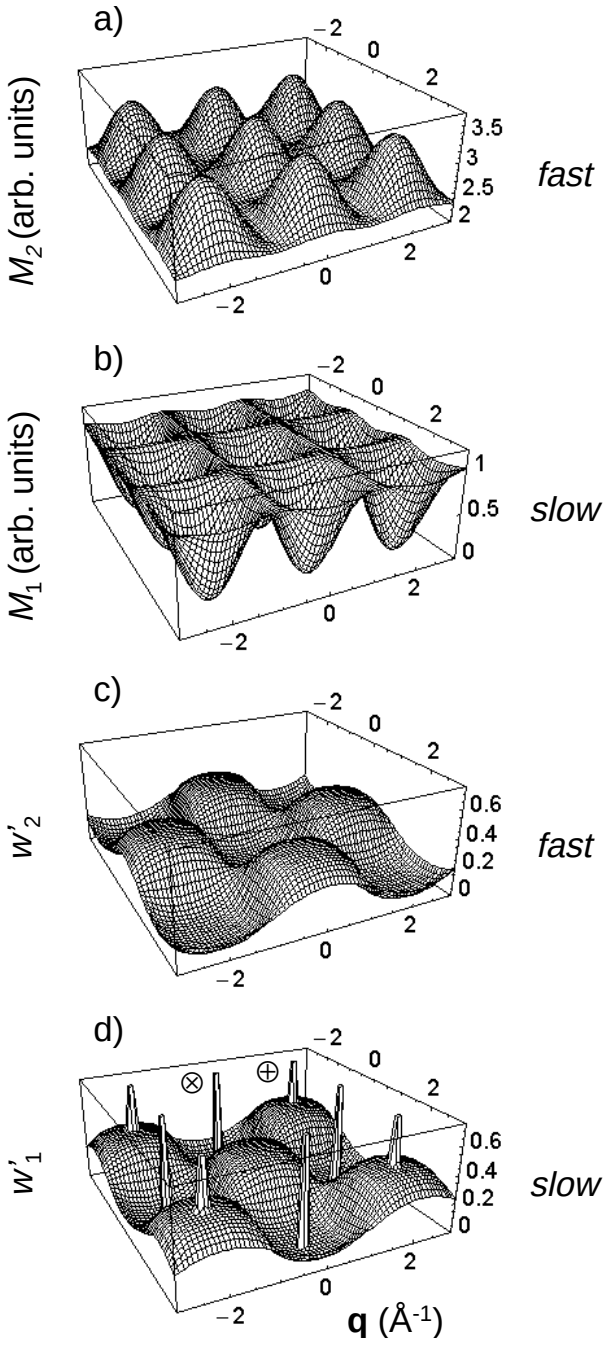

Fig. 6. Representation of the intermediate scattering function along a section in the ⟨001⟩ plane in reciprocal space according to equation (4) for diffusion in a $B2$ system as described in the text. The z-axis of the plots show the decay rates (a,b) and weights (c,d) of the fast (a,c) and the slow (b,d) exponential decay which together constitute the intermediate scattering function. For reciprocal lattice points corresponding to fundamental peaks (⟨110⟩, ⊕) the weights of the fast exponential decay equal zero and the intensity is entirely elastic, for superlattice peaks (⟨100⟩, ⊗) the fast decay has a finite weight corresponding to coherent diffuse scattering. However, the scattered intensity is mainly elastic because the intensity of the broad quasielastic line is small compared to the intensity of the elastic line. The regions between the reciprocal lattice points correspond to quasielastic diffuse scattering due to lattice disorder.

5 Conclusions

A TDI experiment in Bragg directions on the intermetallic alloy $Co_{60}Ga_{40}$ indicates that the high intensities scattered into Bragg directions are mainly elastic. Lower limits for the elastic contribution of 0.94 for the fundamental reflection and 0.75 for the superlattice reflection were found. This result is in accordance with a derivation of the coherent scattering factor using the Van Hove formalism. This scattering function is mainly elastic in Bragg directions except from an underlying isotropic, diffuse component, which is probably too small to be detected. We therefore propose to use diffuse scattering *between* reciprocal lattice points for diffusion studies on crystalline materials. This has been illustrated on the example of a $B2$ structure.

M.K. kindly acknowledges the very helpful discussions with U. van Buerck. This work was financed by the Austrian Fonds zur Förderung der wissenschaftlichen Forschung (FWF), Contract No. P-12492-PHY. H. Thiess acknowledges the support of the Austrian BMWV, Contract No. GZ 616.305/1-III/2/98. Work at the Advanced Photon Source was supported by the U.S. Department of Energy, Basic Energy Sciences, Office of Science, under Contract No. W-31-109-Eng-38.

Appendix A: Two or more scattering components

The coherent scattering function for structures consisting of different scattering elements, contains interference terms from atoms with different atomic scattering factors. This makes an extra indication necessary: Different elements are indicated by m and n, R denotes the total number of elements. Atomic jumps are described by R rate equations, one for each element. Spatial Fourier transformation yields R separate first order differential equations for the intermediate scattering functions. These equations can again be written in matrix notation using R jump matrices $\mathbf{A}_n$ containing jump vectors and frequencies for atoms of type n. Integration yields R equations for $I'(\mathbf{q},t)$. This solution applies to $I_{in}^{jm}(\mathbf{q},t)$ and the integration constant $(K_{in}'^{jm})^p$ can be specified by Fourier transformation of

$$G_{in}'^{jm}(\mathbf{r},0) = (1-c_i^n)\,\delta_{ij}\,\delta_{mn}\,\delta(\mathbf{r}), \qquad \text{(A.1)}$$

the dynamic part of the correlation function $G_{in}^{jm}(\mathbf{r},t)$ which describes the probability of finding an atom of type n at a position $\mathbf{r}$ on sublattice i under the condition that an atom of type m occupies the position $\mathbf{r}=0$ on sublattice j at $t=0$. The integration constants $(K_{in}'^{jm})^p$ and in consequence the $I_{in}'^{jm}$ vanish for $m \neq n$ which leads to a decoupling so that spectra for diffuse scattering can be

$$w'_p = \frac{\{\alpha E(\mathbf{q}) + [1+\tau_{12}M^p(\mathbf{q})]\}\{(1-c_1)\,\alpha E(\mathbf{q}) + (1-c_2)[1+\tau_{12}M^p(\mathbf{q})]\}}{(1+\alpha)\{\alpha E(\mathbf{q})^2 + [1+\tau_{12}M^p(\mathbf{q})]^2\}}\,. \tag{B.3}$$

calculated separately for each component. The dynamic part of the intermediate scattering function can then be written as:

$$I'(\mathbf{q},t) = \sum_{i,j,m} c_{jm} I_{im}^{jm}(\mathbf{q},t). \tag{A.2}$$

Let L be the total number of sublattices, then $I'(\mathbf{q},t)$ is a sum of $L \times R$ Lorentzians. Hence, the time dependent part of the total coherent scattering function can be obtained by calculating the time dependent parts of the intermediate scattering functions for each element separately. The static part of the correlation function vanishes in the rate equations due to detailed balance. All interference between atoms of different kinds are contained in this static part. The corresponding time independent part of the intermediate scattering function is calculated by direct spatial Fourier transformation and yields the static structure factor.

Appendix B: B2-structure

The $B2$ structure (also CsCl structure) consists of two simple cubic lattices where the sites of one lattice are in the center of the cubic unit cell of the other. One sublattice is mainly occupied by A atoms, the other by B atoms. Let us suppose that a $B2$ structure occupied by one sort of scattering atoms with different concentrations c_1 and c_2 on the two sublattices. The hermitized jump matrix is then of the form

$$\mathbf{B} = \frac{1}{8\tau_{12}} \begin{pmatrix} -8 & \sqrt{\alpha}E(\mathbf{q}) \\ \sqrt{\alpha}E(\mathbf{q}) & -8\alpha \end{pmatrix}, \tag{B.1}$$

where $\alpha = \tau_{12}/\tau_{21}$ and $E(\mathbf{q}) = \sum_{k=1}^{8} \exp(\mathrm{i}\mathbf{q}\mathbf{l}^{(k)})$. The intermediate scattering function, $S(\mathbf{q},t)$, is a sum of two exponentials. Their linewidths are proportional to the eigenvalues M_p of the matrix $\mathbf{B}$ and their weights, w_p, have to be calculated from the eigenvectors of $\mathbf{B}$ using equations (4) and (5). The weights are shown in Figure 2 together with the corresponding eigenvalues. The sum of the weights for the quasielastic contribution is $\mathbf{q}$-independent:

$$\sum_{i=1}^{2} w'_i(\mathbf{q}) = \sum_{i=1}^{2} c_i(1-c_i). \tag{B.2}$$

For reciprocal lattice points we expect elastic lines with weights $w_{\mathrm{Bragg}} = (c_1+c_2)^2$ for fundamental peaks and $w_{\mathrm{Bragg}} = (c_1-c_2)^2$ for superlattice peaks. In both cases a very small admixture of quasielastic diffuse scattering is present, however much too small to be measured. The weights w'_p for diffuse scattering on a $B2$ structure read

see equation (*B*.3) *above*.

If the $B2$ lattice is occupied by two types of scattering atoms, as discussed in the Appendix A, four Lorentzians are expected – two for each component.

References

1. G. Vogl, R. Feldwisch, in *Diffusion in Condensed Matter*, edited by J. Kärger, P. Heitjans, R. Haberlandt (Vieweg, Wiesbaden, 1998).
2. R.C. Knauer, J.G. Mullen, Phys. Rev. **174**, 711 (1978).
3. B. Sepiol, A. Meyer, G. Vogl , H. Franz, R. Rüffer, Phys. Rev. B **57**, 10433 (1998).
4. M. Ait-Salem, T. Springer, A. Heidemann, B. Alefeld, Phil. Mag. A **41** 723 (1979).
5. A.Q.R. Baron, H. Franz, A. Meyer, R. Rüffer, A.I. Chumakov, E. Burkel, W. Petry, Phys. Rev. Lett. **79**, 2823 (1997).
6. K. Ruebenbauer, U.D. Wdowik, Phys. Rev. B **58**, 11896 (1998).
7. This has been shown analytically for coherent neutron scattering *e.g.* by D.K. Ross, D.L.T. Wilson, in *Neutron Inelastic Scattering* Vol. 2, (IAEA, Vienna, 1978), p. 383 or T. Springer, D. Richter, in *Methods of Experimental Physics* (Academic Press, 1987).
8. L. Van Hove, Phys. Rev. **95**, 249 (1954).
9. B. Sepiol, M. Kaisermayr, H. Thiess, G. Vogl, E.E. Alp, W. Sturhahn, Hyperfine Interactions **126**, 329 (2000).
10. R.J. Wasilewski, J. Phys. Chem. Solids **29**, 39 (1968).
11. H. Ipser, A. Mikula, W. Schuster, Monatssch. Chem. **120**, 283 (1989).
12. M. Kaisermayr, J. Combet, H. Ipser, H. Schicketanz, B. Sepiol, G. Vogl, Phys. Rev. B **63**, 054303 (2001).
13. N.A. Stolwijk, M. van Gend, H. Bakker, Phil. Mag. A **42**, 783 (1980).
14. M. Kaisermayr, J. Combet, H. Ipser, H. Schicketanz, B. Sepiol, G. Vogl, Phys. Rev. B **61**, 12038 (2000).
15. B. Sepiol, W. Löser, M. Kaisermayr, R. Weinkamer, P. Fratzl, H. Thiess, M. Sladecek, G. Vogl, Defect Diffus. Forum **194–199** (2001, in press).
16. M. Kaisermayr, B. Sepiol, G. Vogl, Physica B **301** (2001, in press).
17. C.T. Chudley, R.J. Elliott, Proc. Phys. Soc. **77**, 353 (1961).
18. J.M. Rowe, K. Sköld, H.E. Flotow, J.J. Rush, J. Phys. Chem. Solids **32**, 41 (1971).
19. R. Kutner, I. Sosnowska, J. Phys. Chem. Solids **38**, 741 (1977).
20. O.G. Randl, B. Sepiol, G. Vogl, R. Feldwisch, K. Schroeder, Phys. Rev. B **49**, 8768 (1994).